LAWRENCE
LIVERMORE
NATIONAL
LABORATORY

LLNL-TR-765370

Magnetic Microcalorimeter (MMC) Gamma Detectors with Ultra-High Energy Resolution

S. Friedrich

January 10, 2019

This work performed under the auspices of the U.S. Department of Energy by Lawrence Livermore National Laboratory under Contract DE-AC52-07NA27344.

Magnetic Microcalorimeter (MMC) Gamma Detectors with Ultra-High Energy Resolution

PI: **Stephan Friedrich, Lawrence Livermore (LLNL)**

Co-I: **Stephen Boyd, University of New Mexico (UNM)**

Robin Cantor, Star Cryoelectronics LLC (STAR Cryo)

Collaborator: **Christian Enss, Heidelberg University**

Project Overview

The goal of this LCP is to develop ultra-high resolution gamma-ray detectors based on magnetic microcalorimeters (MMCs) for accurate measurements of nuclear decay data and NDA of nuclear materials. For highest energy resolution, we are introducing erbium-doped silver (Ag:Er) as a novel sensor material and implement several geometry and design changes to improve the signal-to-noise ratio. The detector sensitivity will be increased by developing arrays of 32 Ag:Er pixels read out by 16 SQUID preamplifiers, and by developing a cryogenic Compton veto to reduce the spectral background. For highest energy resolution we will operate the MMC detector arrays in a dilution refrigerator with a base temperature <10 mK. The detector performance and utility will be demonstrated with radioactive sources of interest to the safeguards community.

In FY16 and FY17, we had purchased a liquid-cryogen-free dilution refrigerator and installed 16 SQUID preamplifiers and writing for MMC detector operation at ~10 mK. We have also developed the process to fabricate the first Ag:Er-based MMCs, built prototype detector arrays and tested them with different radioactive sources. We have also shown that our MMC detectors can achieve the LCP goal of an energy resolution below 50 eV as needed to resolve most closely-spaced lines of interest for NDA.

The goals for FY18 were then 1) to optimize the MMC design based on the measured detector characteristics and to increase the array size to 32-pixels for increased sensitivity, and 2) to demonstrate the utility of MMC gamma-ray detectors in applications relevant in nuclear safeguards.

1) Optimized 32-pixel MMC Gamma Detector Arrays

Our first set of MMC detectors in FY17 had already achieved the LCP goal of an energy resolution of 38 eV FWHM [Boyd 2018]. Still, there were several aspects of the detector performance that could be further improved. Specifically, the power dissipations of the first stage SQUID preamplifiers, which were integrated with the MMCs on the same chip, increased the operating temperature of the MMC above the ~10 mK base temperature of the dilution refrigerator and thereby reduced their energy resolution. In addition, the signal rise time was too fast, so that high-energy gamma-rays would exceed the SQUID slew rate and be no longer detectable. Also, the ~5 ms decay time, while acceptable, should be further increased to allow detector operation at several tens of counts/s per pixel. Finally, the some material parameters such as the heat capacities of the Er-dopants seemed to differ from the expected values. Addressing these shortcomings was not just a matter of academic interest, because any further improvements in resolution can always be traded in for increased pixel size and thus improved efficiency to increase the sensitivity of the MMC detector.

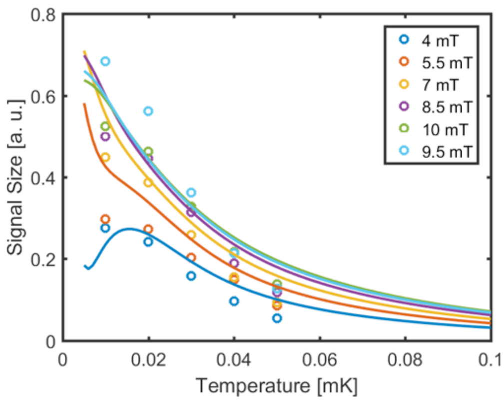

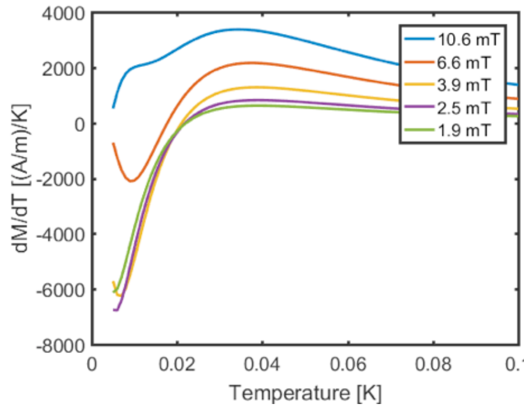

Figure 1 (left): Simulation of gamma signal size as a function of temperature for different applied magnetic fields (solid lines), compared to the values measured in one of our first-generation Ag:Er MMCs (circles). These simulations are used to extract the exact device parameters such as head capacities, thermal conductivities and coupling constants. Figure 2 (right): Simulations for a particular MMC geometry illustrate that the magnetic sensor response to gamma-ray heating (dM/dT) depends sensitively on temperature and applied magnetic field (different colors). Detector optimization is therefore a complicated iterative process constrained by photolithographic capabilities.

It is conceptually straightforward to prevent the SQUID preamplifier from heating the MMC detector by placing the two components onto two separate chips (see Figure 5). The difficulty arises from the increased inductance introduced by the wire bonds between the two chips, which reduces the signal size, increases noise and changes the electronic response of the circuit. Similarly, to prevent high-energy gammas from exceeding the SQUID slew rate, the signal rise time can always be reduced by increasing the absorber size and thus its heat capacity. While this is desirable for increased detection efficiency, it increases noise and may not be compatible with our current fabrication technology. To speed up the MMC response, the signal decay time can be reduced by increasing the width and thus the thermal coupling of the gold bridge between the MMC and the thermal bus, but this risks introducing spatial variations of the response if the rise time varies slightly for different gamma absorption locations within a pixel.

We have therefore performed extensive simulations of the MMC detector response to simultaneously optimize their energy resolution, detection efficiency and count rate based on the data we took in FY17/18, taking into account the photolithographic fabrication capabilities at STAR Cryo. These simulations were conducted at the UNM Center for Supercomputing and are based on a full 3D model of the detectors. They include details such as the magnetic coupling between the Er-dopants to estimate the temperature at which they start to order spontaneously, as well as the ac Josephson effect of the SQUIDs and its influence on device noise.

Figure 1 shows the simulated signal size as a function of temperature for different magnetizing fields and their comparison with the measured data (circles). These types of initial simulations are used to extract the actual material parameters such as heat capacities, thermal conductivities and Er concentrations, which do in general differ from the ideal literature values used in the initial MMC design. Once the simulations are reliable and match the observed detector characteristics, they can be used to predict the device response for new geometries and device configurations (Figure 2).

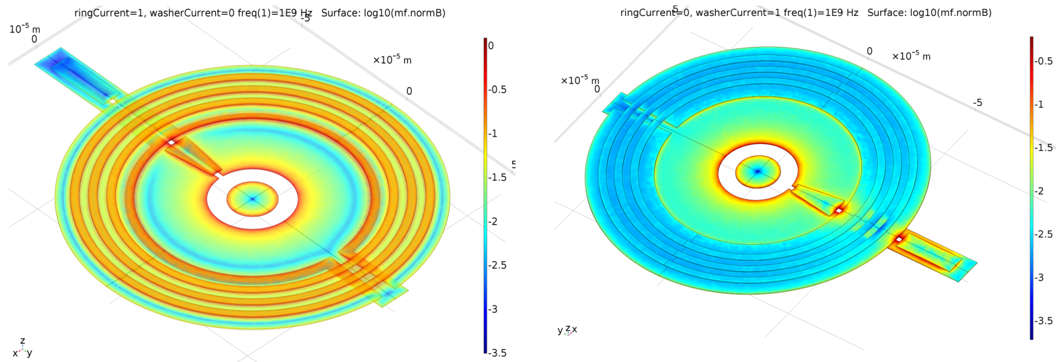

Figure 3 (left): Simulated magnetic fields at the surface of the magnetizing coil, here simplified to three concentric loops (right), and in the SQUID sensor coil (left). Understanding the surface fields helps us to spot and eliminate unintended flux concentrations. Because these calculations are fully 3D, they allow us for the first time to accurately account for non-axisymmetric features such as the leads, a flux-concentrating washer added to reduce capacitive coupling, and three patches added to reduce slit inductance.

A significant effort went into simulating the magnetic coupling between the Ag:Er sensor and the two superconducting Nb coils, one to magnetize the Er dopants and produce a Zeman splitting between the spin states, and one to pick up the magnetic gamma-ray signal and couple it to the SQUID preamplifier. Device geometries are then optimized to maximize the mutual coupling factor and thus the signal transfer (Figure 3).

Based on these simulations, we have developed a final design of MMC pixels that are estimated to have a limiting resolution of ~20 eV FWHM for gamma energies of 100 keV and ~1 ms decay times for maximum count rates of several tens of counts/s per pixel. These pixels have the same cross-sectional structure as the earlier MMCs (Figure 4) and can therefore be fabricated with the same photolithographic processes developed during FY16 and FY17. The full array consists of 32 of these pixels, with groups of 8 pixels read out by individual chips with 4 SQUID preamplifiers each (Figure 5). Fabrication of the arrays will be completed in FY19.

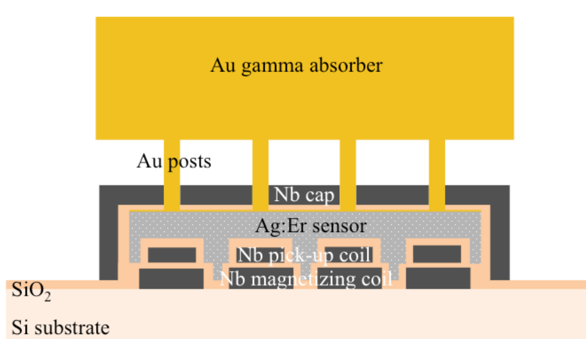

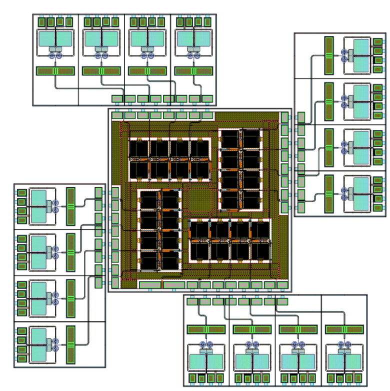

Fig. 4 (left): Schematic cross section of the MMC with the Au gamma-ray absorber supported on top of the Ag:Er sensor by Au posts. Current in the lower Nb coil magnetizes the Er spins in the Ag:Er sensor, and sensor heating by gamma-rays induces a signal in the upper Nb pick-up coil that is coupled into the SQUID preamplifier. Fig. 5 (right): Layout of a central 4×8-pixel MMC array, surrounded by four chips with 4 SQUID preamplifiers each.

2) Detector Performance in Safeguards-Relevant Applications

Ultra-high energy resolution is not the only detector characteristic that is essential for high-accuracy NDA and improved nuclear decay data. In addition to an energy resolution below 50 eV [Boyd 2018], the detector response also must be sufficiently uniform to allow adding spectra from different pixels. And since literature values of nuclear decay data should be independently confirmed by groups at different institutions, it is important that the results from different devices are consistent. We have therefore duplicated the analysis of our $^{233}U/^{239}Pu$ source with two different high-resolution setups, once with MMCs from our Heidelberg collaborators read out with SQUID preamplifiers from Magnicon, and once with MMCs from the University of New Mexico read out with SQUIDs from STAR Cryo (Figure 6). Several pixels from each setup were tested in the same dilution refrigerator, and both sets of signals were read out with the same digitizers and processed with the same trapezoidal filter algorithm.

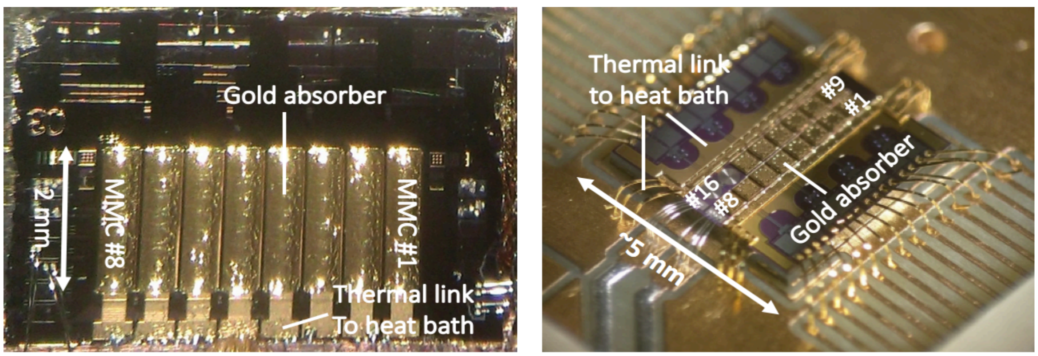

Figure 6: MMC gamma detectors developed at the Kirchhoff Institute of Physics (KIP) at Heidelberg University (left) and at the University of New Mexico (UNM) (right).

We find that both sets of detectors can be calibrated with a simple quadratic response with only a small non-linearity of order $\sim 10^{-4}$ to 10^{-5}/ keV (Figure 7). The UNM detector has a smaller heat capacity, and its non-linearity is therefore slightly larger, as expected. Because of the predictable quadratic response, all gamma-ray energies can be measured with very high accuracy. Most importantly, both sets of detectors provide consistent values of the gamma-ray energies (Figure 8), in the sense that they consistently either agree with the literature values or consistently show a discrepancy. Since both MMC setups observe the same discrepancies with the literature values, the data suggest that the error is in the literature values and not due to a peculiarity of the MMC or SQUID response. This is a significant breakthrough, because it provides confidence that MMCs can be used to improve the literature values of nuclear decay data [Kim 2018].

It is well known that the uncertainty of nuclear decay data can limit the accuracy of NDA in nuclear safeguards [e.g. Bosco 2009]. The energies and branching ratios of the two Th-234 gamma rays at ~92 keV, which are used for accurate non-destructive assay of U enrichment despite their overlap in HPGe spectra, are one example. The literature values of their energies have an error of ±10 and ±20 eV, and their published branching ratios are only known to an accuracy of ±10%. We have therefore prepared a Th-234 source and measured its gamma spectrum with our prototype MMC detectors (Figure 9). Although the energy resolution during that run was “only” ~120 eV FWHM, the two gammas at 92.38(1) and 92.80(2) keV still well resolved (Figure 10). This allowed us to extract the centroid energies with a precision <1 eV, an order of magnitude better than the current literature values [Friedrich 2018].

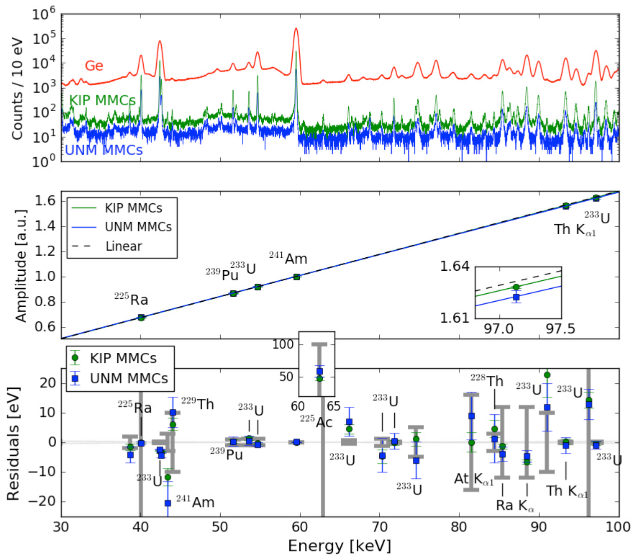

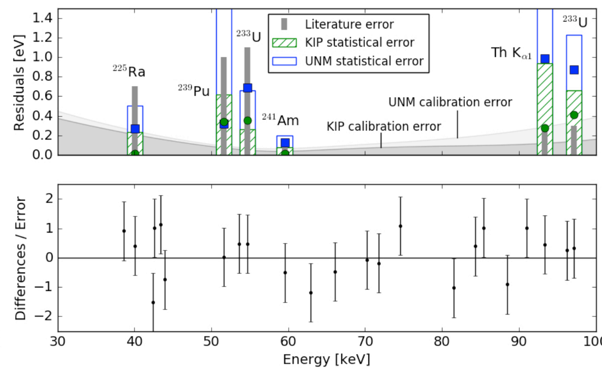

Figure 7 (left): MMC spectra (top), calibration (center) and residuals (bottom) from the same $^{233}U/^{239}Pu$ source, once measured with MMCs from the Heidelberg Kirchhoff Institute for Physics ("KIP MMCs", green) and once taken with MMCs from the University of New Mexico ("UNM MMCs", blue). Both detectors can be calibrated with a simple second-order polynomial, and the non-linearity of the smaller UNM MMCs is larger, as expected (center). The residuals for both MMCs agree for all lines within the error of the measurement, suggesting that non-zero deviations from the literature values are due to a literature error rather than detector artifacts. Figure 8 (right): The precision of the MMC measurements is comparable to the precision of the calibration lines in the literature (top). The difference between the UNM and the KIP MMCs are consistent with the error of the measurement for all lines in the spectrum, i.e. the ratio of difference / error is consistent with zero within the error bar of the measurement (bottom) [Kim 2018].

The problem with these measurements is that the calibration lines used for these spectra have errors significantly above 1 eV. We will therefore not publish updated values for the Th-234 decay data until we have repeated the MMC measurements with a better calibration source and quantified the other systematic errors [Friedrich 2018].

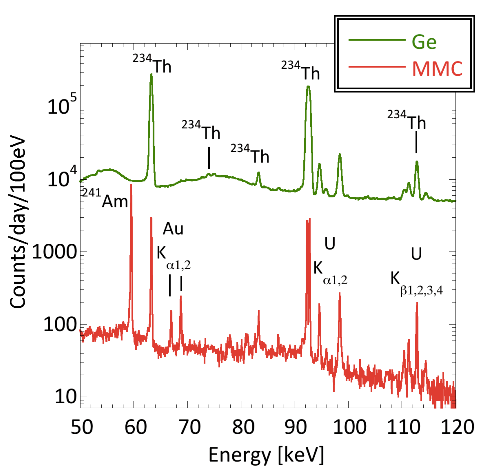

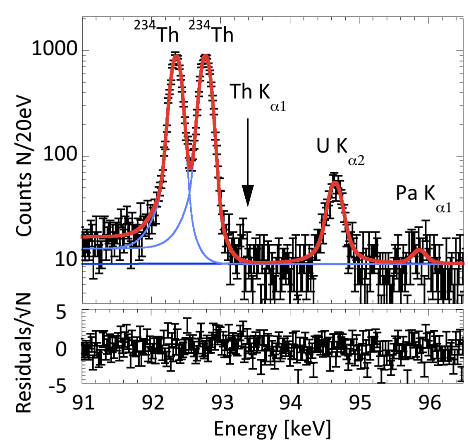

Figure 9 (left): Th-234 spectra from the MMC detectors (red) and a planar Ge detector (green). Figure 10 (right): Despite an energy resolution of "only" 120 eV in this run, the MMC can still resolve the two Th-234 gamma-rays at 92.38 and 92.80 keV. The response function, which has been extracted from the Am-241 line at 60 keV, is constant throughout the spectrum so that a fit matches the spectrum within the accuracy of the measurement [Friedrich 2018].

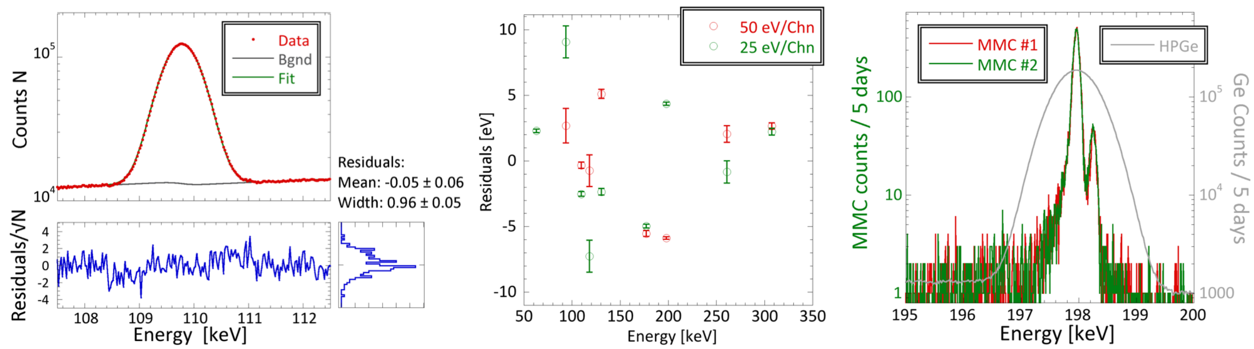

Figure 11 (left): The line shape of modern HPGe detectors matches the theoretically expected Gaussian function on top of an erfc background within the error of the measurement (if the measurement is set up correctly). This is a significant improvement over the line shape of the Ge detectors that were used to generate the decay data of current nuclear libraries. Figure 12 (center): Residuals from the *exact same* Yb-169 data captured with two different MCAs differ significantly. This suggests that non-linearities of the MCA can contribute significantly to the literature values of gamma-ray energies measured with HPGe detectors. Figure 13 (right): MMCs improve centroid measurements because of their narrower linewidth, and they can identify interfering lines that overlap in HPGe spectra, in this case a Tm-169 line at 198.241(1) keV close to the Yb-169 calibration line at 197.95797(60) keV.

Among the possible calibration sources, Yb-169 stands out as the isotope with the best-characterized gamma energies and branching ratios at low energies where most high-accuracy NDA is performed [Helmer 2000]. Unfortunately, Yb-169 is not commercially available. We have therefore produced Yb-169 in the Tm-169(d,2n)Yb-169 reaction by irradiating a Tm film with 15 MeV deuterons at the 88" Cyclotron at LBL. We have then examined this source with modern HPGe detectors, whose line shape can match theoretical expressions rather well (Figure 11), to reproduce some of the literature values from isotopes used for actinide NDA. In this context we have discovered that even modern MCAs introduce non-linearities whose effects exceed the uncertainties of typical literature data (Figure 12). This is one of the errors that have not been considered in the measurements that current data libraries are based on, and we suspect it is one of the reasons why many energy values bars in these libraries are incorrect and many uncertainties are likely underestimated.

We have also tested our MMC gamma detectors with the Yb-169 source (Figure 13) and are currently analyzing these data. We hope that the final procedure we develop will provide a method how to systematically improve nuclear decay data. We intend to summarize the results in a publication that can serve as a guide on how to best measure decay data used for NDA, using both HPGe and MMC gamma detectors.

Summary and Outlook

We have developed magnetic microcalorimeter (MMC) gamma-ray detectors with an energy resolution as good as 38 eV. The most significant result of FY18 was the confirmation that MMC detectors produced by different institution and read out with different SQUID preamplifiers produce spectra that are consistent with one another, and in particular spectra that show consistent discrepancies with the decay data of nuclear libraries. This provides confidence that MMCs can be used to improve the decay data in these libraries and therefore the accuracy of NDA based on these data. Further improvements in sensitivity now require the fabrication of larger arrays, as originally proposed for this LCP, and improvements in (or corrections for) the non-idealities of readout systems.

Since the simulations to optimize the device design took much longer than expected, the fabrication of 32-pixel MMC detector arrays is currently several months behind schedule. We have therefore requested a no-cost extension of this project until 03/31/19 to complete the fabrication of the 32-pixel arrays and test their performance. During that time, we will also continue our experiments with Yb-169 and establish an experimental procedure to improve nuclear decay data and accurately quantify their uncertainties.

References

[Bosco 2009] "Impact of the detector energy resolution on the performance of MGA and MGAU isotopic codes", A. Bosko, S. Croft, S. Philips, R. Gunnink, *J. Radioanal. Nucl. Chem*. **282**, 855–860 (2009)

[Boyd 2018] "Integrated SQUID/Sensor Metallic Magnetic Microcalorimeter for Gamma-Ray Spectroscopy", S. T. P. Boyd, R. Hummatov, G. B. Kim, J. A. Hall, R. Cantor, S. Friedrich, accepted to *J. Low Temp. Phys*. **193**, 435-440 (2018)

[Friedrich 2018] "Magnetic Microcalorimeter Gamma Detectors for High-Accuracy Nuclear Decay Data", S. Friedrich, G.-B. Kim, R. Hummatov, T. Parsons-Davis, R. Cantor, S. Boyd, *Proceedings of the 51st Annual Meeting of the Institute of Nuclear Materials Management,* Baltimore (2018)

[Helmer 2000] "Recommended standards for γ-ray energy calibration (1999)", R. G. Helmer, C. van der Leun, *Nucl. Inst. Meth. A* **450**, 35- 70 (2000)

[Kim 2018] "Consistent measurements of ^{233}U gamma emissions using metallic magnetic calorimeters with ultra-high energy resolution", G.-B. Kim, R. Hummatov, S. Kempf, C. Flynn, R. Cantor, A. Fleischmann, S. T. P. Boyd, C. Enss, S. Friedrich, *J. Radioanal. Nucl. Chem*. **318**, 803-808 (2018)